Hindawi
Wireless Communications and Mobile Computing
Volume 2020, Article ID 2746038, 13 pages
https://doi.org/10.1155/2020/2746038

Research Article

Success Probability Analysis of C-V2X Communications on Irregular Manhattan Grids

Bin Pan and Hao Wu

State Key Laboratory of Rail Traffic Control and Safety, Beijing Jiaotong University, Beijing, China

Correspondence should be addressed to Hao Wu; hwu@bjtu.edu.cn

Received 18 February 2020; Revised 19 July 2020; Accepted 26 July 2020; Published 19 August 2020

Academic Editor: Pavlos I. Lazaridis

To overcome the shortcomings of Dedicated Short Range Communications (DSRC), cellular vehicle-to-everything (C-V2X) communications have been proposed recently, which has a variety of advantages over traditional DSRC, including longer communication range, broader coverage, greater reliability, and smooth evolution path towards 5G. In this paper, we consider an LTE-based C-V2X communications network in irregular Manhattan grids. We model the macrobase stations (MBSs) as a 2D Poisson point process (PPP) and model the roads as a Manhattan Poisson line process (MPLP), with the roadside units (RSUs) modeled as a 1D PPP on each road. As an enhancement architecture to DSRC, C-V2X communications include vehicle-to-vehicle (V2V) communication, vehicle-to-infrastructure (V2I) communication, vehicle-to-pedestrian (V2P) communication, and vehicle-to-network (V2N) communication. Since the spectrum for PC5 interface in 5.9 GHz is quite limited, cellular networks could share some channels to V2I links to improve spectral efficiency. Thus, according to Maximum Power-based Scheme, we adopt the stochastic geometry approach to compute the signal-to-interference ratio- (SIR-) based success probability of a typical vehicle that connects to an RSU or an MBS and the area spectral efficiency of the whole network over shared V2I and V2N downlink channels. In addition, we study the asymptotic characteristics of success probability and provide some design insights according to the impact of several key parameters on success probability.

1. Introduction

Vehicular communication networks are significant components of intelligent transportation system (ITS), which can provide many benefits, such as enhancing road safety, reducing traffic jam, and providing entertainment services. An important solution of this evolution is cellular vehicle-to-everything (C-V2X) communications, which include vehicle-to-vehicle (V2V) communication, vehicle-to-infrastructure (V2I) communication, vehicle-to-pedestrian (V2P) communication, and vehicle-to-network (V2N) communication. V2V communication can promote information sharing among vehicles without network assistance. V2I and V2N communications can enable vehicles to connect with the core network, which offer many services from basic safety messages and entertainment applications to automatic driving. V2P communication enhances the relationship between running vehicles and walking pedestrians. C-V2X enabled by long-term evolution (LTE) communication has been defined by the third generation partnership project (3GPP) as part of Release 14 [1].

Existing vehicular communications are limited by short range, connection interruption, channel congestion, and nonsupporting high-density communication, which is supported by Dedicated Short Range Communications (DSRC) technology [2]. In DSRC-based system, infrastructures consist of roadside units (RSUs), which are sparsely distributed especially in remote areas due to the high cost of deployment. What's more, single DSRC communication is unable to support everincreasing novel on-board applications like automatic driving. Thus, LTE-based C-V2X communication was proposed to overcome the shortcomings of DSRC, which has a variety of advantages over traditional DSRC, including longer communication range, broader coverage, greater reliability, and smooth evolution path towards 5G.

The dissemination of messages in C-V2X system has two kinds of patterns, namely, direct mode and infrastructure mode. In direct mode, vehicles can connect to other vehicles, RSUs, and pedestrians directly over PC5 interface, which are referred to V2V/V2I/V2P links, respectively. As for infrastructure mode, vehicles communicate with cellular networks over Uu interface, which is for V2N link. As there may be large number of vehicles at urban roads and the spectrum for PC5 interface is quite limited, cellular networks can share some channels to V2I links to improve spectral efficiency. In order to analyze the communication quality in C-V2X network, we adopt stochastic geometry approach, which is a powerful tool that has been applied to wireless networks to analyze the mutual interference.

1.1. Related Works. The initial studies using stochastic geometry on vehicular networks are limited to a single road or an intersection [3–7]. In [3], the authors proposed two models based on signal-to-interference plus noise ratio (SINR) and Shannon's law to calculate the optimum transmission probability and transmission range of vehicles on a single road. In [4], the authors proposed a tractable model to study the performance of broadcast protocols with vehicles' locations modeled as a Poisson point process (PPP) in a single road. In [5], the authors proposed a tractable model to study the multihop transmissions for intervehicle communication in a multilane highway scenario, according to stochastic geometry approach. In [6], the authors proposed a tractable and accurate model to calculate the packet reception probability of a specific link in the intersection scenario of vehicular networks. In [7], the authors also presented a model to evaluate the reliability of packet transmissions near intersections of vehicular networks. They provided the closed form expression of the packet reception probability and can be extended to multilane cases.

There is also a little literature focusing on complex road spatial distribution recently. In [8], the authors derived the coverage probability of a typical receiver in vehicular network, which roadways are modeled by Poisson line process (PLP) and the vehicles are modeled by 1D PPP. In [9], the authors proposed a tractable framework of performance analysis of CV2X network over shared cellular and V2V uplink channels and obtained the closed-form expressions for success probability in direct mode and network mode. In [10], the authors analyzed the characteristics of Poisson line Cox point process, which is helpful for network modeling in Internet of Vehicles (IoV). They derived some fundamental properties of the point process, which is useful to quantify the performance of novel vehicular architectures. In particular, a number of researchers pay attention to the orthogonal street system, which is the most common urban road topologies in practice. In [11], the authors focused on the reliability analysis of V2V communications in the regular street system, in which the horizontal and vertical streets have the same fixed intervals. In [12], the authors presented a model for success probability in an urban environment, where the horizontal streets have the same fixed intervals which are different from the intervals of the vertical streets. As far as we know, this paper is the first to calculate the success probability for Manhattan C-V2X network where the intervals of horizontal and vertical streets follow the Poisson distribution. More details of our contributions are followed below.

1.2. Contributions. In this paper, we propose a framework for success analysis of an irregular Manhattan C-V2X network. We model the spatial layout of MBSs as a 2D PPP and model the spatial layout of roads as a Manhattan PLP (MPLP), with the RSUs modeled as a 1D PPP on each road. We choose the general power-law path-loss model and Rayleigh fading to describe the channel effects. For an arbitrarily chosen typical vehicle, we compute the signal-to-interference ratio- (SIR-) based success probability, according to Maximum Power-based Scheme. We also provide useful design insights by studying the impact of key parameters on the success probability. More technical details are as follows.

1.2.1. Success Probability. We derive an accurate expression for SIR-based success probability of a typical vehicle in an irregular Manhattan C-V2X network. We first calculate null probability and fundamental distance distributions, which are useful to calculate the success probability. Next, we derive the Laplace transform of interference from three independent sources. Then, we calculate the association probability and success probability of a typical vehicle according to Maximum Power-based Scheme. We also give the expression for area spectral efficiency and asymptotic characteristics of success probability.

1.2.2. Design Insights. According to our theoretical analysis, we explore the impact of three key network parameters on the success probability. It is observed that the success probability increases with the increase of RSU intensity. However, the success probability decreases with the increase of MBS intensity and road intensity. Therefore, in terms of success probability, we should reduce the use of MBSs while other application requirements for MBSs are met and, meanwhile, increase the deployment intensity of RSUs. As for area spectral efficiency, we also require dense deployment of RSUs to improve it.

2. System Model

2.1. MPLP. We give a brief introduction to MPLP first. As shown in Figure 1, MPLP consists of two types of undirected lines which are orthogonal, namely, horizontal lines and vertical lines. Thus, the spatial layout of these lines in R^2 displays the grid-like structure. Instead of the same fixed values, the intervals between adjacent horizontal or vertical lines are generated by a 1D PPP, respectively. Thereby, to construct a MPLP in R^2, we can first fill points on the x- and y-axes according to two independent 1D PPPs Ξ_x and Ξ_y and then draw vertical and horizontal lines on the basis of these points. According to [13], a MPLP Φ_l is stationary if the 1D PPPs Ξ_x and Ξ_y are stationary, which means the distribution of lines is invariant to any translation $T_{(t,\beta)}$.

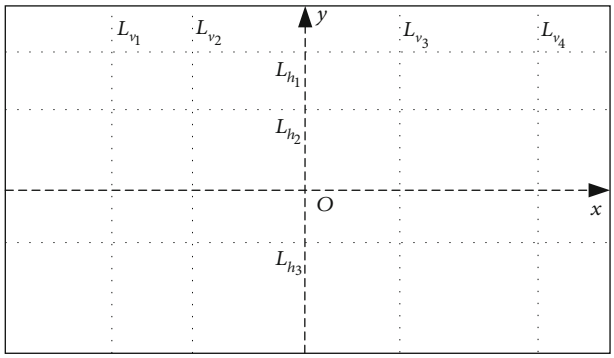

FIGURE 1: Illustration of MPLP in 2D plane R^2.

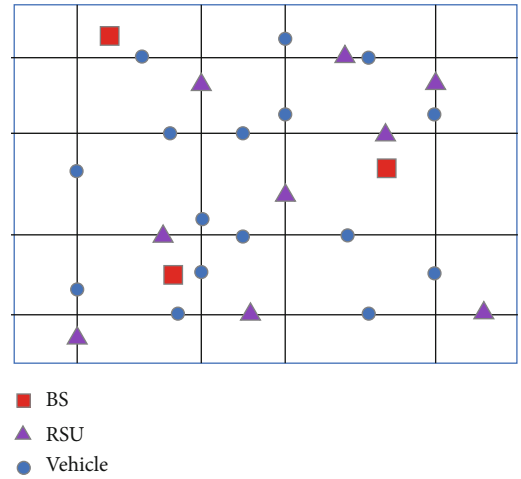

FIGURE 2: System model.

2.2. Spatial Model. As shown in Figure 2, the cellular macro-base stations (MBSs) are randomly distributed in R^2 according to a 2D PPP with intensity λ_c [14, 15]. We model the road network as a stationary MPLP $\Phi_l \equiv \{L_{h1}, L_{h2}, \cdots, L_{v1}, L_{v2} \cdots\}$ in R^2. We denote the set of horizontal and vertical lines by $\Phi_{lh} = \{L_{h1}, L_{h2}, \cdots\}$ and $\Phi_{lv} = \{L_{v1}, L_{v2}, \cdots\}$, which are generated by two independent homogeneous 1D PPPs Ξ_y and Ξ_x with the same intensity λ_l for conciseness of the final expressions. The locations of vehicles are randomly distributed on each road as 1D PPP with intensity λ_v. Since RSUs are deployed along the roadside, the locations of RSUs are also randomly distributed on each road as 1D PPP with the same intensity λ_u. Therefore, driven by the same MPLP Φ_l, the locations of vehicular nodes and RSU nodes can form two Cox processes Φ_v and Φ_u, which are stationary [10, 16]. We name the arbitrary chosen vehicle node in Φ_v as typical vehicle and the road where the typical vehicle located as typical road. There are altogether two types of typical vehicles: (i) typical general vehicle located at arbitrary position in the road and (ii) typical intersection vehicle located at the intersection of a horizontal and vertical road.

Owing to the stationary of Φ_v, we pay attention to the analysis of a typical vehicle at the origin O. Thus, without loss of generality, we take the assumption that the typical general vehicle is located on a horizontal road. Therefore, according to Slivnyak's theorem [17, 18], the translated line process is $\Phi_{l0,\text{gen}} = \Phi_l \cup L_x$. And the resulting point process $\Phi_{v0,\text{gen}}$ is interpreted as the superposition of point process Φ_v, an 1D PPP with intensity λ_v on the x-axis L_x and a point at the origin O. Similarly, as the point process Φ_u is also driven by the same MPLP Φ_l, the resulting point process $\Phi_{u0,\text{gen}}$ is the superposition of the point process Φ_u and a 1D PPP with intensity λ_u on L_x.

In the special case, typical intersection vehicle is located at the intersection of a horizontal line L_x and a vertical line L_y, which correspond to x-axis and y-axis, respectively. Using the same method, under this conditioning, the resulting line process is $\Phi_{l0,\text{int}} = \Phi_l \cup \{L_x, L_y\}$. Therefore, the resulting point process $\Phi_{v0,\text{int}}$ is interpreted as the superposition of point process Φ_v, two independent 1D PPPs each with intensity λ_v on L_x and L_y, and a point at the origin o. In the same way, the resulting point process $\Phi_{u0,\text{int}}$ can be translated as the superposition of Φ_u and two independent 1D PPPs each with intensity λ_u along L_x and L_y, respectively. For these two types of typical vehicles, we can apply the similar approach to calculate their success probabilities. Thus, we only give the details for typical general vehicle. In the rest of this paper, typical vehicle refers to typical general vehicle for simplicity of exposition.

The number of horizontal and vertical lines that intersect a region $A \subset R^2$ is denoted by $N_{lh}(A)$ and $N_{lv}(A)$, respectively. And the number of points in set A is denoted by $N_p(A)$.

2.3. Transmitter Association Scheme. The vehicles in the network select to connect to either an MBS or an RSU according to Maximum Power-based Scheme. In this scheme, the vehicle connects to the transmitter (an MBS or an RSU) from which it receives the highest average power.

The vehicle chooses the closest RSU and MBS first and then selects to receive data from the one that can supply a higher time-average power.

To find the received power, we should introduce the channel model next. We use a general power-law path-loss model with exponent $\alpha > 2$ to describe the long time-scale channel effects. To describe the short time-scale channel effects, we use the Rayleigh fading in which the channel gain is exponentially distributed with unit mean. Thus, the instantaneous power received can be expressed by $P_{\text{rec}} = Phr^{-\alpha}$, where P is the transmit power, $h \sim \exp(1)$ models Rayleigh fading, and r is the distance between transmitter and receiver. We use time-average value of received power as the metric to choose transmitter, because it is undesirable to switch from one transmitter to another frequently due to the rapidly varying instantaneous power. If the average time interval is much larger than the coherence time of channel, the average received power is considered to be independent of h, which can be given by $P_{\text{av}} = Pr^{-\alpha}$. We assume all MBSs have the same transmit power P_c, and all RSUs have the same transmit power P_u.

3. Success Probability

3.1. Null Probability

Lemma 1. *Null probability of RSU: for a MPLP Φ_l, which are generated by two independent homogeneous 1D PPPs with the same intensity λ_l and RSUs lie on each road followed by 1D PPP with intensity λ_u, the probability that there is no RSUs inside a disk $b(o,R)$ is*

$$\mathbb{P}(N_u(b(o,R))=0)=\exp\left[-4\lambda_l\left(\int_0^R 1-e^{-2\lambda_u\sqrt{R^2-r^2}}dr\right)\right]. \tag{1}$$

Proof. The null probability can be calculated as

$$\begin{aligned}
\mathbb{P}(N_u(b(o,R))=0) &\overset{(a)}{=} \mathbb{P}(N_u(\Phi_{lh}\cap b(o,R))=0)\\
&\quad\times\mathbb{P}(N_u(\Phi_{lv}\cap b(o,R))=0)\\
&\overset{(b)}{=}\left[\sum_{n=0}^{\infty}\mathbb{P}(N_{lh}(b(o,R))=n)\times\prod_{i=1}^{n}\mathbb{P}\left(N_u\left(L_{h_i}\cap b(o,R)\right)=0\right)\right]\\
&\quad\times\left[\sum_{n=0}^{\infty}\mathbb{P}(N_{lv}(b(o,R))=n)\times\prod_{i=1}^{n}\mathbb{P}\left(N_u\left(L_{v_i}\cap b(o,R)\right)=0\right)\right]\\
&=\left[\sum_{n=0}^{\infty}\frac{e^{-2\lambda_l R}(2\lambda_l R)^n}{n!}\left(\int_{-R}^{R}e^{-2\lambda_u\sqrt{R^2-r^2}}\frac{1}{2R}dr\right)^n\right]^2\\
&=\left[e^{-2\lambda_l R}\sum_{n=0}^{\infty}\frac{\left(\lambda_l\int_{-R}^{R}e^{-2\lambda_u\sqrt{R^2-r^2}}dr\right)^n}{n!}\right]^2\\
&=\left[e^{-2\lambda_l R}\exp\left(2\lambda_l\int_0^R e^{-2\lambda_u\sqrt{R^2-r^2}}dr\right)\right]^2\\
&=\exp\left[-4\lambda_l\left(\int_0^R 1-e^{-2\lambda_u\sqrt{R^2-r^2}}dr\right)\right],
\end{aligned} \tag{2}$$

where (a) follows from that there is no RSU on both horizontal and vertical roads and the distribution of horizontal and vertical roads are independent, and (b) follows from conditioning over the number of horizontal and vertical roads inside the disk.

3.2. Distance Distribution.

We derive the distance distributions to the closest RSU and MBS, respectively, which will be used in calculating the success probability.

Lemma 2. *The cumulative distribution function (CDF) and probability distribution function (PDF) of the distance d_u between the typical vehicle and its closest RSU are CDF:*

$$CDF:\ F_{d_u}(\rho)=1-\exp\left(-4\lambda_l\int_0^{\rho}1-e^{-2\lambda_u\sqrt{\rho^2-r^2}}dr\right)e^{-2\lambda_u\rho}, \tag{3}$$

$$\begin{aligned}
PDF:\ f_{d_u}(\rho)&=\exp\left(-4\lambda_l\int_0^{\rho}1-e^{-2\lambda_u\sqrt{\rho^2-r^2}}dr\right)\\
&\quad\times\left(2\lambda_u e^{-2\lambda_u\rho}+8\lambda_u\lambda_l\rho e^{-2\lambda_u\rho}\int_0^{\rho}\frac{e^{-2\lambda_u\sqrt{\rho^2-r^2}}}{\sqrt{\rho^2-r^2}}dr\right).
\end{aligned} \tag{4}$$

Proof. The CDF of d_u can be computed as $F_{d_u}(\rho)=\mathbb{P}(d_u\le\rho)=1-\mathbb{P}(d_u>\rho)$

$$\begin{aligned}
F_{d_u}(\rho)&=\mathbb{P}(d_u\le\rho)=1-\mathbb{P}(d_u>\rho)=\mathbb{P}(d_u\le\rho)\\
&=1-\mathbb{P}(d_u>\rho)\overset{(a)}{=}1-\mathbb{P}(N_u(b(o,\rho))=0)\\
&\quad\cdot\mathbb{P}(N_u(L_x\cap b(o,\rho))=0)\\
&=1-\exp\left(-4\lambda_l\int_0^{\rho}1-e^{-2\lambda_u\sqrt{\rho^2-r^2}}dr\right)e^{-2\lambda_u\rho},
\end{aligned} \tag{5}$$

where (a) follows from that the event $d_u>\rho$ occurs when both of the following independent events occur simultaneously: (i) there is no RSU on Φ_l inside the disk $b(o,\rho)$ and (ii) there is no RSU on L_x inside the disk $b(o,\rho)$. The PDF is derived by differentiating the CDF as follows:

$$\begin{aligned}
f_{d_u}(\rho)&=\frac{\mathrm{d}}{\mathrm{d}\rho}\left[1-\exp\left(-4\lambda_l\int_0^{\rho}1-e^{-2\lambda_u\sqrt{\rho^2-r^2}}dr\right)e^{-2\lambda_u\rho}\right]\\
&=-\frac{\mathrm{d}}{\mathrm{d}\rho}\exp\left(-4\lambda_l\int_0^{\rho}1-e^{-2\lambda_u\sqrt{\rho^2-r^2}}dr\right)e^{-2\lambda_u\rho}\\
&\overset{(a)}{=}\exp\left(-4\lambda_l\int_0^{\rho}1-e^{-2\lambda_u\sqrt{\rho^2-r^2}}dr\right)\\
&\quad\times\left(2\lambda_u e^{-2\lambda_u\rho}+8\lambda_u\lambda_l\rho e^{-2\lambda_u\rho}\int_0^{\rho}\frac{e^{-2\lambda_u\sqrt{\rho^2-r^2}}}{\sqrt{\rho^2-r^2}}dr\right),
\end{aligned} \tag{6}$$

where (a) follows from the Leibniz rule and the differentiation of a definite integral with respect to a parameter.

Lemma 3. *The cumulative distribution function (CDF) and probability distribution function (PDF) of the distance d_c between the typical vehicle and its closest MBS are*

$$CDF:\ F_{d_c}(\rho)=1-e^{-\pi\lambda_c\rho^2}, \tag{7}$$

$$PDF:\ f_{d_c}(\rho)=2\pi\lambda_c\rho e^{-\pi\lambda_c\rho^2}. \tag{8}$$

Proof. The CDF of d_c can be computed as

$$\begin{aligned}
F_{d_c}(\rho)&=\mathbb{P}(d_c\le\rho)=1-\mathbb{P}(d_c>\rho)=1-\mathbb{P}(N_c(b(o,\rho))=0)\\
&=1-e^{-\pi\lambda_c\rho^2}.
\end{aligned} \tag{9}$$

The PDF can be obtained by differentiating the CDF.

3.3. Laplace Transform of Interference.

We first give the expression of Laplace transform of interference under Rayleigh fading, since the success probability can be reduced

to the Laplace transform of interference I, which is a well-known approach [14, 18]. For a wireless network with interfering nodes generated by a PPP Φ, the Laplace transform can be calculated as

$$\begin{aligned} L_I(s) &= \mathbb{E}\left[\exp\left(-\sum_{x\in\Phi} sPh_x\|x\|^{-\alpha}\right)\right] \\ &= \mathbb{E}\left[\prod_{x\in\Phi} E_{h_x}\exp\left(-sPh_x\|x\|^{-\alpha}\right)\right] \\ &= \mathbb{E}\left[\prod_{x\in\Phi}\frac{1}{1+sP\|x\|^{-\alpha}}\right], \end{aligned} \tag{10}$$

where P is the transmit power of each node and $h_x \sim \exp(1)$.

Note that the interference at a typical vehicle are from three independent sources: (i) RSU nodes on the other roads (denoted by Φ_u), (ii) RSU nodes on typical road L_x (denoted by Φ_{ux}), and (iii) MBS nodes (denoted by Φ_c). Thus, the interference from these three sources can be denoted by I_u, I_{ux}, and I_c, respectively. We will calculate the Laplace transform of these interferences below.

Since the typical vehicle always connects to the closest RSU or MBS, we define some distances r_u, r_{ux}, and r_c, which are the minimum distance between typical vehicle and the closest RSU on the other roads, the closest RSU on typical road L_x, and the closest MBS.

Lemma 4. *The Laplace transform of interference distribution from the RSUs on a single road (which is at a distance r) is*

$$L_{I_u}(s, r_u, r) = \begin{cases} g_1(r) = \exp\left[-2\lambda_u\int_0^{+\infty} 1 - \frac{1}{1+sP_u(r^2+t^2)^{-\alpha/2}}dt\right], & r \geq r_u, \\ g_2(r) = \exp\left[-2\lambda_u\int_{\sqrt{r_u^2-r^2}}^{+\infty} 1 - \frac{1}{1+sP_u(r^2+t^2)^{-\alpha/2}}dt\right], & r < r_u. \end{cases} \tag{11}$$

Proof. As shown in Figure 3, there are two roads inside a disk. One is at a distance $r > r_u$ (denoted by D_1), which means the interfering RSUs can be located anywhere on D_1. The other one is at a distance $r < r_u$ (denoted by D_2), which means the interfering RSUs can be only located in the segment $t = (-\sqrt{r_u^2-r^2}, -\sqrt{R^2-r_u^2})$ and $t = (\sqrt{r_u^2-r^2}, \sqrt{R^2-r_u^2})$. Next, we will analyze these two roads, respectively.

The Laplace transform of interference distribution from D_1 is derived by conditioning on the number of points on this line. Given a line at a perpendicular distance r from the center o, the length of the chord inside a disk (with radius R) can be expressed by $2\sqrt{R^2-r^2}$. Thus, the probability of that there are m points on this chord is $e^{-2\lambda_u\sqrt{R^2-r^2}}((2\lambda_u\sqrt{R^2-r^2})^m/m!)$, according to the properties of PPP. Therefore, the

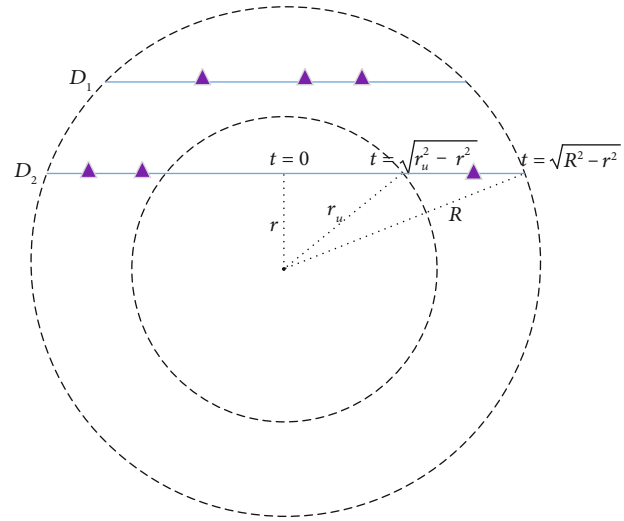

Figure 3: Distribution of interference RSUs on roads.

Laplace transform of total interference in the case of $r \geq r_v$ can be calculated by

$$\begin{aligned} g_1(s, r_u, r) &= \mathbb{E}\left(\prod_{x\in D_r}\frac{1}{1+sP_u\|x\|^{-\alpha}}\right) \\ &= \sum_{m=0}^{\infty}\mathbb{P}(N=m)\left(\int_{-\sqrt{R^2-r^2}}^{\sqrt{R^2-r^2}}\frac{1}{1+sP_u(r^2+t^2)^{-\alpha/2}}f(t)dt\right)^m \\ &= \sum_{m=0}^{\infty}\left[e^{-2\lambda_u\sqrt{R^2-r^2}}\frac{\left(2\lambda_u\sqrt{R^2-r^2}\right)^m}{m!}\right. \\ &\quad\left.\times\left(\int_{-\sqrt{R^2-r^2}}^{\sqrt{R^2-r^2}}\frac{1}{1+sP_u(r^2+t^2)^{-\alpha/2}}\frac{1}{2\sqrt{R^2-r^2}}dt\right)^m\right] \\ &= e^{-2\lambda_u\sqrt{R^2-r^2}}\exp\left[2\lambda_u\int_0^{\sqrt{R^2-r^2}}\frac{1}{1+sP_u(r^2+t^2)^{-\alpha/2}}dt\right] \\ &= \exp\left[-2\lambda_u\int_0^{\sqrt{R^2-r^2}}1-\frac{1}{1+sP_u(r^2+t^2)^{-\alpha/2}}dt\right], \end{aligned} \tag{12}$$

where D_r refers to a road at a perpendicular distance r from the center o. Similarly, the Laplace transform of total interference in the case of $r < r_v$ can be calculated by

$$g_2(s, r_u, r) = \exp\left[-2\lambda_u\int_{\sqrt{r_u^2-r^2}}^{\sqrt{R^2-r^2}}1-\frac{1}{1+sP_u(r^2+t^2)^{-\alpha/2}}dt\right]. \tag{13}$$

The final expressions can be obtained as the radius approaches positive infinity ($R \longrightarrow +\infty$) in (12) and (13).

Lemma 5. *The Laplace transform of total interference from all other roads can be calculated as follows:*

$$L_{I_u}(s, r_u) = \exp\left[-4\lambda_l\left(\int_0^{r_u} 1 - g_2(r)dr + \int_{r_u}^{+\infty} 1 - g_1(r)dr\right)\right]. \tag{14}$$

Proof. The Laplace transform of total interference from all other roads can be calculated as

$$\begin{aligned} L_{I_u}(s, r_u) &= \mathbb{E}\left[e^{-sI_u}\right] = \mathbb{E}\left[e^{-s\mathbb{E}\left[\sum_{x\in\Phi_u} I(x)\right]}\right] \\ &= \mathbb{E}\left[\prod_{x\in\Phi_u} e^{-s\mathbb{E}[I(x)]}\right] \overset{(a)}{=} \mathbb{E}\left[\prod_{x\in\Phi_{u_h}} e^{-s\mathbb{E}[I(x)]}\right] \\ &\times \mathbb{E}\left[\prod_{x\in\Phi_{u_v}} e^{-s\mathbb{E}[I(x)]}\right] = \left[\sum_{j=0}^{\infty} \frac{e^{-2r_u\lambda_l}(2r_u\lambda_l)^j}{j!}\left(\int_{-r_u}^{r_u} \frac{g_2(r)}{2r_u}dr\right)^j\right. \\ &\left.\times \sum_{k=0}^{\infty} \frac{e^{-2(R-r_u)\lambda_l}[2(R-r_u)\lambda_l]^k}{k!}\left(\int_{r_u}^{R} \frac{g_1(r)}{(R-r_u)}dr\right)^k\right]^2 \\ &= \exp\left[-4\lambda_l\left(\int_0^{r_u} 1 - g_2(r)dr + \int_{r_u}^{R} 1 - g_1(r)dr\right)\right], \end{aligned} \tag{15}$$

where (a) refers to the fact that the total interference are from the RSUs on horizontal and vertical roads, which are independent and identically distributed (i.i.d.). The final expression can be obtained as the radius approaches positive infinity ($R \longrightarrow +\infty$) in (15).

Lemma 6. *The Laplace transform of total interference from the typical road L_x can be calculated as follows:*

$$L_{I_{u_x}}(s, r_{u_x}) = \exp\left(-2\lambda_u \int_{r_{u_x}}^{+\infty} 1 - \frac{1}{1 + sP_u t^{-\alpha}}dt\right). \tag{16}$$

Proof. We have obtained the Laplace transform of interference from the RSUs on a single node in Lemma 4. Therefore, the Laplace transform of interference from all the RSUs on L_x can be derived by substituting $r = 0$ and $r_u = r_{ux}$, respectively, in $g_2(r)$.

The expression of Laplace transform L_{Ic} from the interference MBSs with a 2D PPP can be derived by [19]:

$$L_{I_c}(s, r_c) = \exp\left[-2\pi\lambda_c \int_{r_c}^{+\infty} \left(1 - \frac{1}{1 + sP_c r^{-\alpha}}\right) r dr\right]. \tag{17}$$

The total interference at origin o is the sum of three types of interference sources, i.e.,

$$I = I_u + I_{u_x} + I_c. \tag{18}$$

As these three types of interference sources are independent with each other, the Laplace transform of the total interference can be given by:

$$L_I(s, r_u, r_{u_x}, r_c) = L_{I_u}(s, r_u) L_{I_{u_x}}(s, r_{u_x}) L_{I_c}(s, r_c). \tag{19}$$

3.4. Association Probability. In Maximum Power-based Scheme, the typical vehicle aims to connect to the transmitter from which it could receive the strongest signal (i.e., average received power). In other words, the typical vehicle chooses to receive signal from the closest RSU or the closest MBS, which can supply a higher time-average power.

To derive the overall success probability, we first should calculate the probability of the typical vehicle connecting to RSU and MBS, respectively.

Lemma 7. *The probability of an RSU being the transmitter at a distance of ρ from the typical vehicle can be calculated by*

$$\mathbb{P}_u(\rho) = \exp\left(-\lambda_c \pi d_{uc}^2\right), \tag{20}$$

where $d_{uc} = (P_c/P_u)^{1/\alpha}\rho$.

Proof. A typical vehicle connects to the closest RSU when the average received power from it is larger than that from the closest MBS. Thus, given the distance between the vehicle and its closest RSU and MBS (d_u and d_c), the probability of this event occurring can be expressed by

$$\mathbb{P}(P_u d_u^{-\alpha} > P_c d_c^{-\alpha}) = \mathbb{P}\left[d_c > \left(\frac{P_c}{P_u}\right)^{1/\alpha} d_u\right]. \tag{21}$$

Let $d_{uc} = (P_c/P_u)^{1/\alpha} d_u$ for simplicity of notation. Therefore, the typical vehicle at origin o connects to the closest RSU when there is no MBS existing in the disk $b(o, d_{uc})$, which happens with the probability

$$\mathbb{P}_u(d_u) = \exp\left(-\lambda_c \pi d_{uc}^2\right). \tag{22}$$

As the typical vehicle connects to the closest RSU, substitute $d_u = \rho$. Thus, we can obtain the result.

Lemma 8. *The probability of an MBS being the transmitter at a distance of ρ from the typical vehicle can be calculated by*

$$\mathbb{P}_c(\rho) = \exp\left[-4\lambda_l\left(\int_0^{d_{cu}} 1 - e^{-2\lambda_u\sqrt{d_{cu}^2 - r^2}}dr\right)\right] e^{-2\lambda_u d_{cu}}, \tag{23}$$

where $d_{cu} = (P_u/P_c)^{1/\alpha}\rho$.

Proof. Following the same method as in Lemma 7, the probability of this event occurring is

$$\mathbb{P}(P_c d_c^{-\alpha} > P_u d_u^{-\alpha}) = \mathbb{P}\left[d_u > \left(\frac{P_u}{P_c}\right)^{1/\alpha} d_c\right]. \tag{24}$$

Let $d_{cu} = (P_u/P_c)^{1/\alpha} d_c$ for simplicity of notation. The typical vehicle at origin o connects to the closest MBS when there is no RSU existing on Φ_l and L_x in the disk $b(o, d_{cu})$, which happens with the probability

$$\begin{aligned}\mathbb{P}_c(d_c) &= \mathbb{P}[N_u(b(o, d_{cu})) = 0]\mathbb{P}[N_u(L_x \cap b(o, d_{cu})) = 0] \\ &= \exp\left[-4\lambda_l\left(\int_0^{d_{cu}} 1 - e^{-2\lambda_u\sqrt{d_{cu}^2 - r^2}} dr\right)\right] e^{-2\lambda_u d_{cu}}.\end{aligned} \tag{25}$$

As the typical vehicle connects to the closest MBS, substitute $d_c = \rho$. Thus, we can obtain the result.

Thus, given the association probabilities conditioned on the value of ρ in Lemmas 7 and 8, the overall probabilities of associating with the closest RSU and closest MBS can be calculated by

$$\mathbb{P}_u = \int_0^{+\infty} \mathbb{P}_u(\rho) f_{d_u}(\rho) d\rho, \tag{26}$$

$$\mathbb{P}_c = \int_0^{+\infty} \mathbb{P}_c(\rho) f_{d_c}(\rho) d\rho. \tag{27}$$

3.5. Success Probability. In this paper, we use SIR as the metric to judge whether to receive message successfully. If the SIR measured at typical vehicle is larger than a predefined threshold β, the message can be detected successfully. Thus, the success probability in a Rayleigh fading network can be derived by

$$\begin{aligned}\mathbb{P}_{\text{suc}} &= \mathbb{P}(\text{SIR} > \beta) = \mathbb{P}\left(\frac{Ph\rho^{-\alpha}}{I} > \beta\right) = \mathbb{P}\left(h > \frac{\beta\rho^{\alpha} I}{P}\right) \\ &= \mathbb{E}\left[\exp\left(-\frac{\beta\rho^{\alpha} I}{P}\right)\right] = L_I\left(\frac{\beta\rho^{\alpha}}{P}\right).\end{aligned} \tag{28}$$

Therefore, the success probability can be expressed by the Laplace transform of interference ($L_I(s)$, where $s = \beta\rho^{\alpha}/P$).

When the typical vehicle connects to the closest RSU at a distance ρ, there is no interfering RSU on Φ_l in the disk $b(o, \rho)$ and on typical road L_x in segment $[-\rho, \rho]$, and no MBS in the disk $b(o, d_{uc})$, i.e., $r_u = \rho, r_{ux} = \rho, r_c = d_{uc}$.

Lemma 9. *The success probability that the typical vehicle connects to the closest RSU, which is at a distance of ρ, can be expressed by:*

$$\mathbb{P}_{suc|u}(\rho) = L_{I_u}\left(\frac{1}{P_u}\beta\rho^{\alpha}, \rho\right) L_{I_{u_x}}\left(\frac{1}{P_u}\beta\rho^{\alpha}, \rho\right) \times L_{I_c}\left(\frac{1}{P_u}\beta\rho^{\alpha}, d_{uc}\right). \tag{29}$$

When the typical vehicle connects to the closest MBS at a distance ρ, there is no interfering RSU on Φ_l in the disk $b(o, d_{cu})$ and on typical road L_x in segment $[-d_{cu}, d_{cu}]$, and no MBS in the disk $b(o, \rho)$, i.e., $r_u = d_{cu}, r_{ux} = d_{cu}, r_c = \rho$.

Lemma 10. *The success probability that the typical vehicle connects to the closest MBS, which is at a distance of ρ, can be expressed by*

$$\mathbb{P}_{suc|c}(\rho) = L_{I_u}\left(\frac{1}{P_c}\beta\rho^{\alpha}, d_{cu}\right) L_{I_{u_x}}\left(\frac{1}{P_c}\beta\rho^{\alpha}, d_{cu}\right) \times L_{I_c}\left(\frac{1}{P_c}\beta\rho^{\alpha}, \rho\right). \tag{30}$$

Note that the expressions for L_{Iu}, L_{Iux}, and L_{Ic} can be obtained from the results in Equations (14), (16), and (17).

Theorem 11. *The total success probability at a typical vehicle in C-V2X networks is*

$$\begin{aligned}\mathbb{P}_{suc} = &\int_0^{+\infty} \mathbb{P}_u(\rho)\mathbb{P}_{suc|u}(\rho) f_{d_u}(\rho) \\ &\cdot d\rho + \int_0^{+\infty} \mathbb{P}_c(\rho)\mathbb{P}_{suc|c}(\rho) f_{d_c}(\rho) d\rho,\end{aligned} \tag{31}$$

where the first term and second term can be named as $P_{suc,u}$ and $P_{suc,c}$, which mean the probabilities of the typical vehicle connecting to an RSU and MBS successfully, respectively.

Proof. The total success probability can be calculated as

$$\begin{aligned}\mathbb{P}_{\text{suc}} &= \mathbb{E}_{\rho}\left[\mathbb{P}_u(\rho)\mathbb{P}_{\text{suc}|u}(\rho) + \mathbb{P}_c(\rho)\mathbb{P}_{\text{suc}|c}(\rho)\right] \\ &\overset{(a)}{=} \int_0^{+\infty} \mathbb{P}_u(\rho)\mathbb{P}_{\text{suc}|u}(\rho) f_{d_u}(\rho) \\ &\quad \cdot d\rho + \int_0^{+\infty} \mathbb{P}_c(\rho)\mathbb{P}_{\text{suc}|c}(\rho) f_{d_c}(\rho) d\rho,\end{aligned} \tag{32}$$

where (a) follows from the fact that success probability for RSU or MBS can be derived by taking an expectation over ρ.

3.6. Area Spectral Efficiency. Area spectral efficiency can be defined by the average bits transmitted per unit time per unit bandwidth per unit area, which can be calculated by

$$\text{ASE} = \lambda_a \log(1 + \beta)\mathbb{P}_{\text{suc},u} + \lambda_c \log(1 + \beta)\mathbb{P}_{\text{suc},c}, \tag{33}$$

where λ_a is the intensity of vehicle nodes in R^2 given by $\lambda_a = \mu_l\lambda_v$, and μ_l is the line density which can be calculated by $\mu_l = 2\lambda_l$ for a stationary MPLP [13].

3.7. Asymptotic Characteristic

Lemma 12. *As the MBS intensity approaches zero ($\lambda_c \longrightarrow 0$), the association probability with the closest $\mathbb{P}_u^{(\lambda_c \to 0)}$ is 1, the association probability with the closest MBS $\mathbb{P}_c^{(\lambda_c \to 0)}$ is 0, and the success probability is*

$$\mathbb{P}_{suc}^{(\lambda_c \to 0)} = \int_0^{+\infty} L_{I_u}\left(\frac{1}{P_u}\beta\rho^{\alpha}, \rho\right) L_{I_{ux}}\left(\frac{1}{P_u}\beta\rho^{\alpha}, \rho\right) f_{d_u}(\rho)d\rho. \tag{34}$$

Proof. By applying the limit $\lambda_c \longrightarrow 0$ on P_u, we can obtain

$$\begin{aligned}\mathbb{P}_u^{(\lambda_c \to 0)} &= \lim_{\lambda_c \to 0} \mathbb{P}_u = \lim_{\lambda_c \to 0} \int_0^R \mathbb{P}_u(\rho) f_{d_u}(\rho) \\ &\cdot d\rho \overset{(a)}{=} \int_0^{+\infty} \lim_{\lambda_c \to 0} \mathbb{P}_u(\rho) f_{d_u}(\rho) \\ &\cdot d\rho = \int_0^{+\infty} 1 \cdot f_{d_u}(\rho)d\rho = 1,\end{aligned} \tag{35}$$

where (a) follows from applying Dominated Convergence Theorem (DCT). Using the similar approach, we can obtain $\mathbb{P}_c^{(\lambda_c \to 0)}$ and $\mathbb{P}_{\text{suc}}^{(\lambda_c \to 0)}$.

Remark 13. As the MBS intensity approaches zero ($\lambda_c \longrightarrow 0$), it can be reduced to a traditional vehicular network without MBS deployment. Thus, the association probability with the closest RSU is equal to 1, and the total interference are all from the other RSU nodes.

Lemma 14. *As the road intensity approaches zero ($\lambda_l \longrightarrow 0$), the association probability with the closest RSU is*

$$\mathbb{P}_u^{(\lambda_l \to 0)} = \int_0^{+\infty} \mathbb{P}_u(\rho) 2\lambda_u e^{-2\lambda_u \rho} d\rho, \tag{36}$$

the association probability with the closest MBS is

$$\mathbb{P}_c^{(\lambda_l \to 0)} = \int_0^{+\infty} e^{-2\lambda_u d_{cu}} f_{d_c}(\rho)d\rho, \tag{37}$$

and the success probability is

$$\begin{aligned}\mathbb{P}_{suc}^{(\lambda_l \to 0)} = &\int_0^{+\infty} \mathbb{P}_u(\rho) L_{I_{ux}}\left(\frac{1}{P_u}\beta\rho^{\alpha}, \rho\right) \\ &\times L_{I_c}\left(\frac{1}{P_u}\beta\rho^{\alpha}, d_{uc}\right) 2\lambda_u e^{-2\lambda_u \rho} d\rho \\ &+ \int_0^{+\infty} e^{-2\lambda_u d_{cu}} L_{I_{ux}}\left(\frac{1}{P_c}\beta\rho^{\alpha}, d_{cu}\right) \\ &\times L_{I_c}\left(\frac{1}{P_c}\beta\rho^{\alpha}, \rho\right) f_{d_c}(\rho)d\rho.\end{aligned} \tag{38}$$

Proof. The details is omitted, as the method is the same as that in Lemma 12.

Remark 15. As the road intensity approaches zero ($\lambda_l \longrightarrow 0$), it can be reduced to a highway scenario with only one road. Thus, the association node can only be selected between the RSUs on the typical road and surrounding MBSs.

Lemma 16. *As the road intensity approaches positive infinity ($\lambda_l \longrightarrow +\infty$) and the RSU intensity approaches to 0 ($\lambda_u \longrightarrow 0$) while the overall intensity of RSUs is constant ($2\lambda_l\lambda_u = \lambda_a$), the association probability with the closest RSU is*

$$\mathbb{P}_u^{(\lambda_l \to +\infty)} = \int_0^{+\infty} \mathbb{P}_u(\rho) f_{d_u}^{(\lambda_l \to +\infty)}(\rho)d\rho, \tag{39}$$

the association probability with the closest MBS is

$$\mathbb{P}_c^{(\lambda_l \to +\infty)} = \int_0^{+\infty} \mathbb{P}_c^{(\lambda_l \to +\infty)}(\rho) f_{d_c}(\rho)d\rho, \tag{40}$$

and the success probability is

$$\begin{aligned}P_{suc} = &\int_0^{+\infty} P_u(\rho) L_{I_u}^{(\lambda_l \to +\infty)}\left(\frac{1}{P_u}\beta\rho^{\alpha}, \rho\right) \\ &\times L_{I_c}\left(\frac{1}{P_u}\beta\rho^{\alpha}, d_{uc}\right) f_{d_u}^{(\lambda_l \to +\infty)}(\rho)d\rho \\ &+ \int_0^{+\infty} P_c^{(\lambda_l \to +\infty)}(\rho) L_{I_u}^{(\lambda_l \to +\infty)}\left(\frac{1}{P_c}\beta\rho^{\alpha}, d_{cu}\right) \\ &\times L_{I_c}\left(\frac{1}{P_c}\beta\rho^{\alpha}, \rho\right) f_{d_c}(\rho)d\rho.\end{aligned} \tag{41}$$

Proof. By applying the limits $\lambda_l \longrightarrow +\infty$ and $\lambda_u \longrightarrow 0$ with $\lambda_a = 2\lambda_l\lambda_u$ unchanged, the asymptotic null probability in Lemma 1 can be calculated by

$$\begin{aligned}&\lim_{\lambda_l \to +\infty} \mathbb{P}(N_u(b(0,R)) = 0) \\ &= \lim_{\lambda_l \to +\infty} \exp\left[-4\lambda_l\left(\int_0^R 1 - e^{-2\lambda_u\sqrt{R^2-r^2}}dr\right)\right] \\ &\overset{(a)}{=} \exp\left[\lim_{\lambda_l \to +\infty} -4\lambda_l\left(\int_0^R 1 - e^{-2(\lambda_a/2\lambda_l)\sqrt{R^2-r^2}}dr\right)\right] \\ &\overset{(b)}{=} \exp\left[\lim_{\lambda_l \to +\infty} 4\lambda_l\left(\int_0^R \sum_{k=1}^{+\infty} \frac{\left(-(\lambda_a/\lambda_l)\sqrt{R^2-r^2}\right)^k}{k!}dr\right)\right] \\ &= \exp\left[\lim_{\lambda_l \to +\infty} 4\lambda_l\left(\int_0^R -\frac{\lambda_a}{\lambda_l}\sqrt{R^2-r^2}dr\right) + \lim_{\lambda_l \to +\infty} 4\lambda_l\right. \\ &\quad \left.\times\left(\int_0^R \sum_{k=2}^{+\infty} \frac{\left(-(\lambda_a/\lambda_l)\sqrt{R^2-r^2}\right)^k}{k!}dr\right)\right] \\ &\overset{(c)}{=} \exp\left(\lim_{\lambda_l \to +\infty} -4\lambda_a\int_0^R \sqrt{R^2-r^2}dr\right) = e^{-\pi R^2\lambda_a},\end{aligned} \tag{42}$$

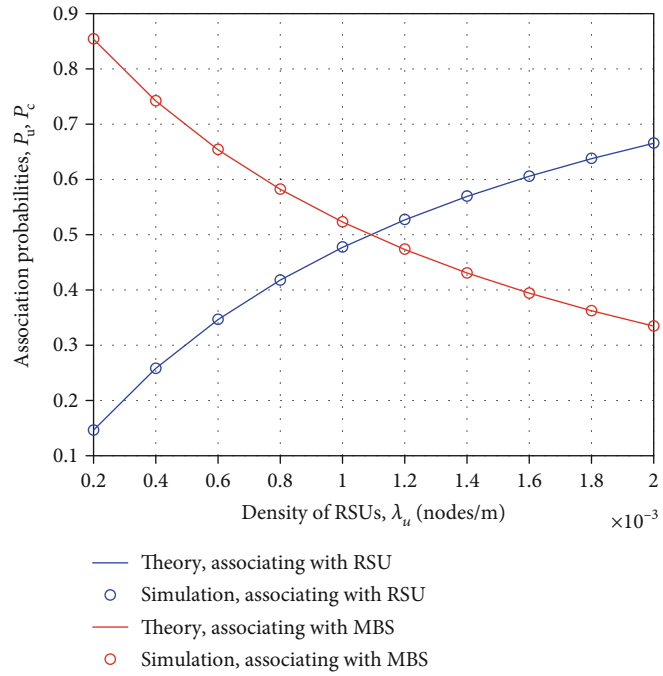

FIGURE 4: Association probabilities with RSU and MBS of the typical vehicle ($\lambda_c = 0.5 \times 10^{-6}$ nodes/m^2, $\lambda_l = 1 \times 10^{-3}$ m^{-1}, and $\beta = 0$ dB).

where (a) follows from substituting $\lambda_u = \lambda_a/2\lambda_l$, (b) follows from the Taylor series expansion of exponential function, and (c) follows from the Dominated Convergence Theorem on the second term, and the limit of the integrand is equal to 0 for $k \geq 2$.

Thus, the cox process Φ_u approaches to a 2D PPP with the intensity λ_a. The PDF of distance d_u between the typical vehicle and its closest RSU can be expressed by

$$f_{d_u}^{(\lambda_l \to +\infty)}(\rho) = 2\pi\lambda_a \rho e^{-\lambda_a \pi \rho^2}. \tag{43}$$

The Laplace transform of total interference from RSUs can be calculated by

$$L_{I_u}^{(\lambda_l \to +\infty)}(s, r_u) = \exp\left[-2\pi\lambda_a \int_{r_u}^{+\infty} \left(1 - \frac{1}{1 + sP_u r^{-\alpha}}\right) r dr\right]. \tag{44}$$

The probability of an MBS being the transmitter at a distance of ρ from the typical vehicle can be calculated by

$$\mathbb{P}_c^{(\lambda_l \to +\infty)}(\rho) = \exp\left(-\lambda_a \pi d_{cu}^2\right). \tag{45}$$

Therefore, the overall probabilities of associating with the closest RSU and closest MBS can be calculated by

$$\mathbb{P}_u^{(\lambda_l \to +\infty)} = \int_0^{+\infty} \mathbb{P}_u(\rho) f_{d_u}^{(\lambda_l \to +\infty)}(\rho) d\rho, \tag{46}$$

$$\mathbb{P}_c^{(\lambda_l \to +\infty)} = \int_0^{+\infty} \mathbb{P}_c^{(\lambda_l \to +\infty)}(\rho) f_{d_c}(\rho) d\rho, \tag{47}$$

and the success probability is

$$\begin{aligned}\mathbb{P}_{\text{suc}} = &\int_0^{+\infty} \mathbb{P}_u(\rho) L_{I_u}^{(\lambda_l \to +\infty)}\left(\frac{1}{P_u}\beta\rho^\alpha, \rho\right) \\ &\times L_{I_c}\left(\frac{1}{P_u}\beta\rho^\alpha, d_{uc}\right) f_{d_u}^{(\lambda_l \to +\infty)}(\rho) d\rho \\ &+ \int_0^{+\infty} \mathbb{P}_c^{(\lambda_l \to +\infty)}(\rho) L_{I_u}^{(\lambda_l \to +\infty)}\left(\frac{1}{P_c}\beta\rho^\alpha, d_{cu}\right) \\ &\times L_{I_c}\left(\frac{1}{P_c}\beta\rho^\alpha, \rho\right) f_{d_c}(\rho) d\rho.\end{aligned} \tag{48}$$

4. Numerical Results and Discussions

We verify the accuracy of our theoretical analysis through Monte Carlo simulations in this section. We will also analyze and discuss the impact of network parameters on success probability, which can give some design insights to network deployment. For all the numerical results in this paper, we assume that the MBSs' transmit power $P_c = 10$ W (40 dBm), the RSUs' transmit power $P_u = 0.1$ W (20 dBm), and the path-loss exponent $\alpha = 4$.

4.1. Association Probability. We first simulate the association probabilities of the typical vehicle with $\lambda_c = 0.5 \times 10^{-6}$ nodes/m^2, $\lambda_l = 1 \times 10^{-3}$ m^{-1}, and $\beta = 0$ dB. From Figure 4, we observe the simulation results are very close to analytical results, which means that our analytical results are accurate. In addition, given a certain λ_u, the sum of these two probabilities is always equal to 1, which indirectly verifies our analytical model is effective. We can also see that the probability of associating with RSUs increases with the increase of RSU intensity, because the

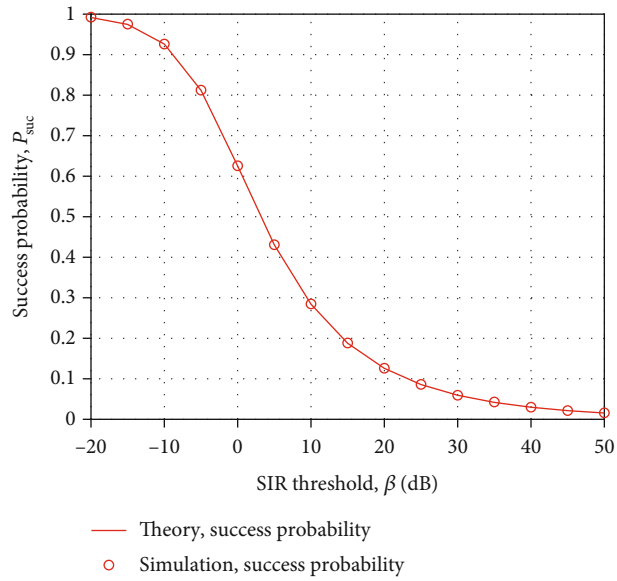

Figure 5: Success probability of the typical vehicle ($\lambda_c = 0.5 \times 10^{-6}$ nodes/m^2, $\lambda_l = 1 \times 10^{-3}$ m^{-1}, and $\lambda_u = 1 \times 10^{-3}$ nodes/m).

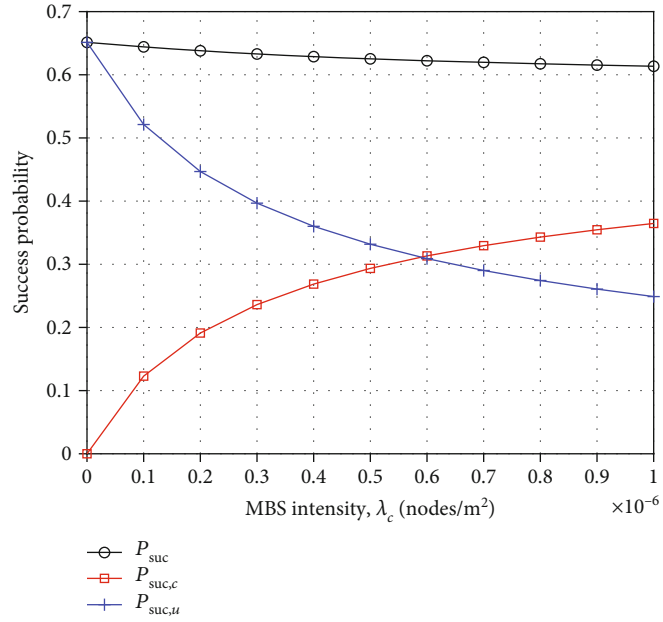

Figure 6: Impact of MBS intensity on success probability ($\lambda_l = 1 \times 10^{-3}$ m^{-1}, $\lambda_u = 1 \times 10^{-3}$ nodes/m, and $\beta = 0$ dB).

typical vehicle will have a higher probability to connect with the surrounding RSUs. The probability of associating with MBSs has the opposite trend.

4.2. Success Probability. We simulate the success probability of the typical vehicle with $\lambda_c = 0.5 \times 10^{-6}$ nodes/m^2, $\lambda_l = 1 \times 10^{-3}$ m^{-1}, and $\lambda_u = 1 \times 10^{-3}$ nodes/m. Figure 5 shows that the simulation results match exactly with the analytical results, which means our analytical results about success probability is accurate. In addition, as shown in Figure 5, the success probability of the typical vehicle decreases with the increase of SIR threshold, which accords with common sense.

4.2.1. Impact of Intensity of MBS. We calculate the success probability of the typical vehicle for road intensity of $\lambda_l = 1 \times 10^{-3}$ m^{-1}, RSU intensity of $\lambda_u = 1 \times 10^{-3}$ nodes/m, SIR threshold of $\beta = 0$ dB, and different MBS intensities. Figure 6 shows that the success probability decreases as the MBS intensity increases. This is because as the MBS intensity increases, the increment of success probability that typical vehicle connects to MBSs is less than the

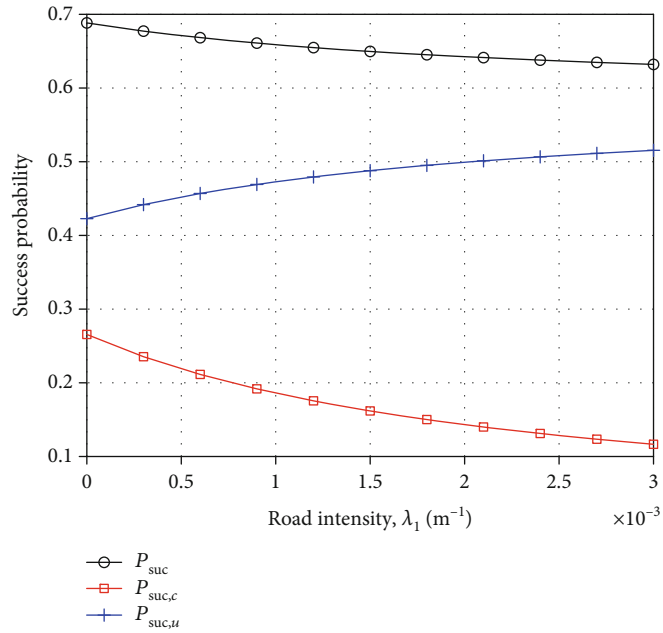

Figure 7: Impact of road intensity on success probability ($\lambda_c = 0.5 \times 10^{-6}$ nodes/m^2, $\lambda_u = 2 \times 10^{-3}$ nodes/m, and $\beta = 0$ dB).

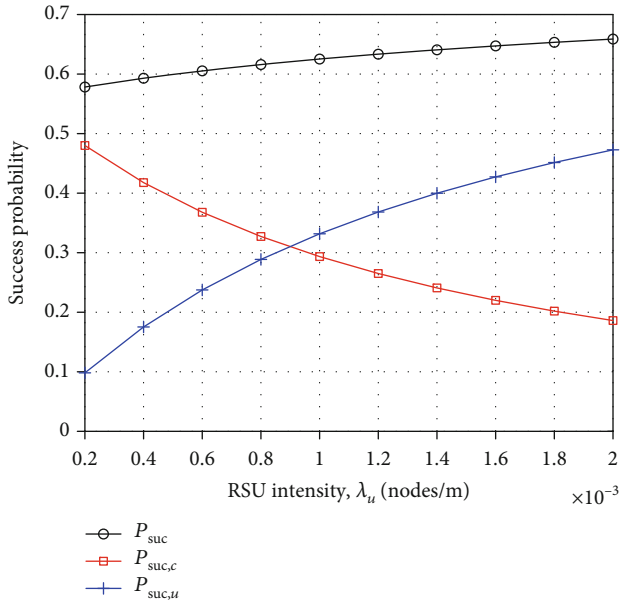

Figure 8: Impact of RSU intensity on success probability ($\lambda_c = 0.5 \times 10^{-3}$ nodes/m^2, $\lambda_l = 1 \times 10^{-3}$ m^{-1}, and $\beta = 0$ dB).

decrement of success probability that typical vehicle connects to RSUs and then affects the total success probability. Therefore, in terms of success probability, we should reduce the use of MBSs as far as possible, when other application requirements are met.

4.2.2. Impact of Intensity of Road. We calculate the success probability of the typical vehicle for MBS intensity of $\lambda_c = 0.5 \times 10^{-6}$ nodes/m^2, RSU intensity of $\lambda_u = 1 \times 10^{-3}$ nodes/m, SIR threshold of $\beta = 0$ dB, and different road intensities. From Figure 7, we can see that the success probability decreases with the increase of road intensity. This trend can be understood that as the road intensity increases, the increment of success probability that typical vehicle connects to RSUs is less than the decrement of success probability that typical vehicle connects to MBSs, as shown in Figure 7. Thus, there is a lower success probability in dense Manhattan block.

4.2.3. Impact of Intensity of RSU. We calculate the success probability of the typical vehicle for MBS intensity of $\lambda_c = 0.5 \times 10^{-6}$ nodes/m^2, road intensity of $\lambda_l = 1 \times 10^{-3}$ m^{-1}, SIR threshold of $\beta = 0$ dB, and different RSU intensities. Different from the features of the impact of MBS intensity and road intensity on success probability, it is observed from Figure 8 that the success probability increases with the increase of the RSU intensity. It is because that the increment of success probability that typical vehicle connects to RSUs is larger than the decrement of success probability that typical vehicle connects to MBSs, as shown in Figure 8. Therefore, to improve success probability, the simplest and most effective way is to increase the deployment intensity of RSUs.

4.2.4. Asymptotic Characteristic of Success Probability. In Figure 9, we plot the success probability of the typical vehicle for several certain values of road intensities and RSU intensities, which satisfy $\lambda_a = 2\lambda_l \times \lambda_u = 2 \times 10^{-6}$ nodes/m^2.

According to the discussions above, we know that the success probability decreases with the increase of road intensity and the decrease of RSU intensity. When road intensity approaches positive infinity ($\lambda_l \to +\infty$) and RSU intensity approaches 0 ($\lambda_u \to 0$), it provides a lower bound for success probability given a certain value of MBS intensity.

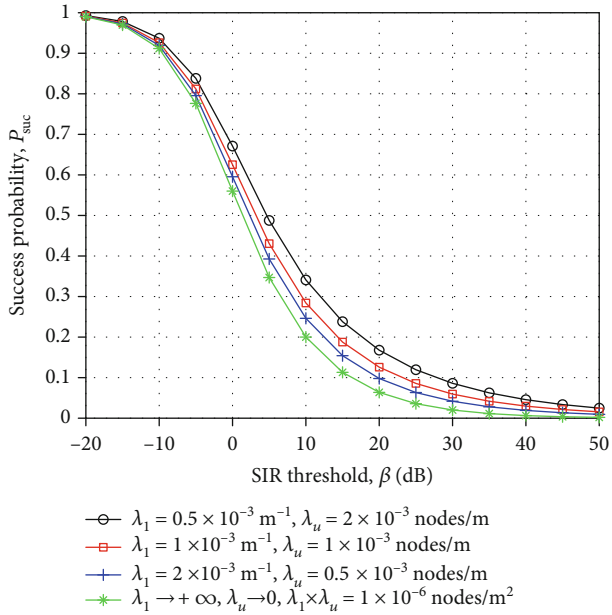

Figure 9: Asymptotic characteristic of success probability ($\lambda_c = 0.5 \times 10^{-3}$ nodes/m^2).

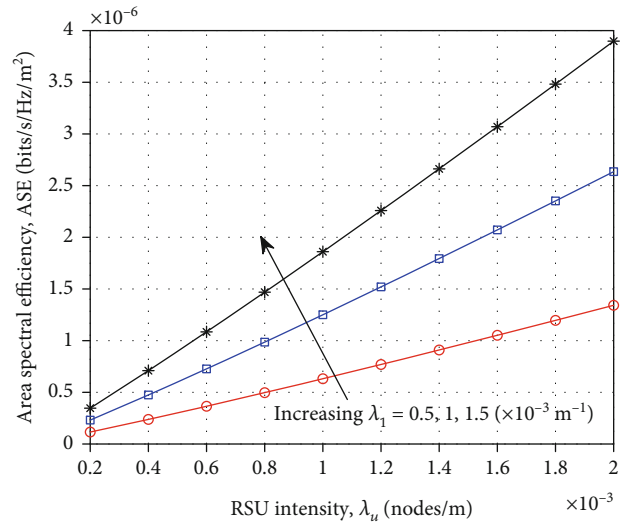

Figure 10: Area spectral efficiency ($\lambda_c = 0.5 \times 10^{-3}$ nodes/m^2).

4.3. Area Spectral Efficiency. We also analyze the impact of road intensity and RSU intensity on area spectral efficiency. As shown in Figure 10, we see that the area spectral efficiency increases with the increase of RSU intensity or the increase of road intensity. It is because as the RSU intensity or road intensity increases, the increment of λ_u or λ_l is much larger than the changes of $P_{suc,u}$ and $P_{suc,c}$ in (33). Thus, the total area spectral efficiency shows an upward trend. Thereby, for the areas with sparse distribution of roads, we can increase the deployment intensity of RSUs to improve area spectral efficiency.

5. Conclusion

In this paper, we derived the success probability of a CV2X communication networks in irregular Manhattan grids over shared downlink channels, according to Maximum Power-based Scheme. We modeled the locations of MBSs as a 2D PPP, the layout of roads as MPLP, and the locations of RSUs as a 1D PPP on each road. We also gave the expression for area spectral efficiency of the whole network and asymptotic characteristic of success probability. What's more, we studied the impact of several key parameters on success probability. It is observed that the success probability increases with the increase of RSU intensity, while it decreases with the increase of MBS and road intensity. Therefore, in terms of success probability, we should reduce the use of MBSs while other application requirements for MBSs are met and, meanwhile, increase the deployment intensity of RSUs. There are several extensions of this work. A more realistic channel model in urban scenario should be considered. Another meaningful issue is to focus on the handover rate of a moving vehicle, including the handover between MBSs, RSUs, and MBS and RSU. In addition, correcting the spatial road model according to the realistic roads in physical environment is worth to be done in the future.

Data Availability

The data used to support the findings of this study are available from the corresponding author upon reasonable request.

Conflicts of Interest

None of the authors have any conflicts of interest.

Acknowledgments

This paper is supported by the State Key Laboratory of Rail Traffic Control and Safety (Contract No. RCS2019ZT006), Beijing Jiaotong University, and it is supported in part by the National Natural Science Foundation of China Grant 61971030.

References

[1] 3GPP, *Document tr 36.885, Study On Lte-Based v2x Services (Release 14), Technical Specification Group Services System*, 3GPP, 2016.

[2] K. Abboud, H. A. Omar, and W. Zhuang, "Interworking of dsrc and cellular network technologies for v2x communications: a survey," *IEEE Transactions on Vehicular Technology*, vol. 65, no. 12, pp. 9457–9470, 2016.

[3] B. Blaszczyszyn, P. Muhlethaler, and Y. Toor, "Maximizing throughput¨ of linear vehicular ad-hoc networks (vanets)—a stochastic approach," in *2009 European Wireless Conference*, pp. 32–36, Aalborg, Denmark, 2009.

[4] S. Busanelli, G. Ferrari, and R. Gruppini, "Performance analysis of broadcast protocols in vanets with poisson vehicle distribution," in *2011 11th International Conference on ITS Telecommunications*, pp. 133–138, St. Petersburg, Russia, 2011.

[5] M. J. Farooq, H. ElSawy, and M.-S. Alouini, "A stochastic geometry model for multi-hop highway vehicular communication," *IEEE Transactions on Wireless Communications*, vol. 15, no. 3, pp. 2276–2291, 2016.

[6] M. Ni, M. Hu, Z. Wang, and Z. Zhong, "Packet reception probability of vanets in urban intersecton scenario," in *2015 International Conference on Connected Vehicles and Expo (ICCVE)*, pp. 124-125, Shenzhen, China, 2015.

[7] E. Steinmetz, M. Wildemeersch, T. Q. Quek, and H. Wymeersch, "A stochastic geometry model for vehicular communication near intersections," in *2015 IEEE Globecom Workshops (GC Wkshps)*, pp. 1–6, San Diego, CA, USA, 2015.

[8] V. V. Chetlur and H. S. Dhillon, "Coverage analysis of a vehicular network modeled as cox process driven by poisson line process," *IEEE Transactions on Wireless Communications*, vol. 17, no. 7, pp. 4401–4416, 2018.

[9] M. N. Sial, Y. Deng, J. Ahmed, A. Nallanathan, and M. Dohler, "Stochastic geometry modeling of cellular v2x communication over shared channels," *IEEE Transactions on Vehicular Technology*, vol. 68, no. 12, pp. 11873–11887, 2019.

[10] C.-S. Choi and F. Baccelli, "Poisson cox point processes for vehicular networks," *IEEE Transactions on Vehicular Technology*, vol. 67, no. 10, pp. 10160–10165, 2018.

[11] J. P. Jeyaraj and M. Haenggi, "Reliability analysis of v2v communications on orthogonal street systems," in *GLOBECOM 2017 - 2017 IEEE Global Communications Conference*, pp. 1–6, Singapore, 2017.

[12] T. Kimura, H. Saito, H. Honda, and R. Kawahara, "Modeling urban its communication via stochastic geometry approach," in *2016 IEEE 84th Vehicular Technology Conference (VTC-Fall)*, pp. 1–5, Montreal, QC, Canada, 2016.

[13] V. V. Chetlur, H. S. Dhillon, and C. P. Dettmann, "Characterizing shortest paths in road systems modeled as manhattan poisson line processes," 2018, https://arxiv.org/abs/1811.11332.

[14] J. G. Andrews, F. Baccelli, and R. K. Ganti, "A tractable approach to coverage and rate in cellular networks," *IEEE Transactions on Communications*, vol. 59, no. 11, pp. 3122–3134, 2011.

[15] S. Mukherjee, "Distribution of downlink sinr in heterogeneous cellular networks," *IEEE Journal on Selected Areas in Communications*, vol. 30, no. 3, pp. 575–585, 2012.

[16] F. Morlot, "A population model based on a poisson line tessellation," in *2012 10th International Symposium on Modeling and Optimization in Mobile, Ad Hoc and Wireless Networks (WiOpt)*, pp. 337–342, Paderborn, Germany, Germany, 2012.

[17] S. N. Chiu, D. Stoyan, W. S. Kendall, and J. Mecke, *Stochastic Geometry and its Applications*, John Wiley & Sons, 2013.

[18] M. Haenggi, *Stochastic Geometry for Wireless Networks*, Cambridge University Press, 2012.

[19] J. G. Andrews, A. K. Gupta, and H. S. Dhillon, "A primer on cellular network analysis using stochastic geometry," 2016, https://arxiv.org/abs/1604.03183.